

# Advances in the use of spiders for direct spinning of nanomaterials-reinforced bionic silk

Cite as: APL Mater. 10, 101111 (2022); <https://doi.org/10.1063/5.0095960>

Submitted: 14 April 2022 • Accepted: 16 September 2022 • Published Online: 31 October 2022

 Gabriele Greco,  Luca Valentini and  Nicola M. Pugno



View Online



Export Citation



CrossMark

## ARTICLES YOU MAY BE INTERESTED IN

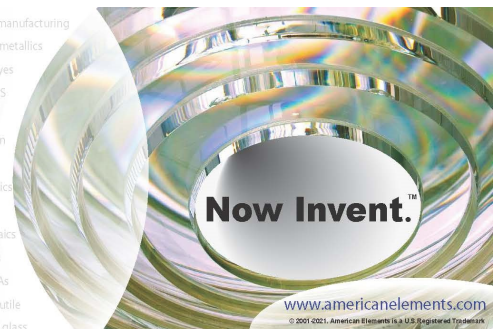
[Pyrocyling-the technique to generate electricity from plastic waste](#)

AIP Conference Proceedings **2494**, 070011 (2022); <https://doi.org/10.1063/5.0106354>



yttrium iron garnet glassy carbon beamsplitters fused quartz additive manufacturing  
 zeolites III-IV semiconductors gallium lump copper nanoparticles organometallics  
 nano ribbons barium fluoride europium phosphors photonics infrared dyes  
 epitaxial crystal growth ultra high purity materials transparent ceramics CIGS  
 cerium oxide polishing powder surface functionalized nanoparticles MRE grade materials thin film  
 OLED lighting solar energy sputtering targets fiber optics  
 h-BN deposition slugs CVD precursors photovoltaics  
 metamaterials borosilicate glass  
 YBCO superconductors InGaAs  
 indium tin oxide MgF<sub>2</sub> rutile  
 diamond micropowder optical glass

The Next Generation of Material Science Catalogs



# Advances in the use of spiders for direct spinning of nanomaterials-reinforced bionic silk

Cite as: *APL Mater.* **10**, 101111 (2022); doi: [10.1063/5.0095960](https://doi.org/10.1063/5.0095960)  
Submitted: 14 April 2022 • Accepted: 16 September 2022 •  
Published Online: 31 October 2022



Gabriele Greco,<sup>1,a)</sup>  Luca Valentini,<sup>2</sup>  and Nicola M. Pugno<sup>1,3,b)</sup> 

## AFFILIATIONS

<sup>1</sup>Laboratory for Bioinspired, Bionic, Nano, Meta, Materials and Mechanics, Department of Civil, Environmental and Mechanical Engineering, University of Trento, Via Mesiano, 77, 38123 Trento, Italy

<sup>2</sup>Department of Civil and Environmental Engineering, University of Perugia and INSTM Research Unit, Strada di Pentima 4, 05100 Terni, Italy

<sup>3</sup>School of Engineering and Materials Science, Queen Mary University of London, Mile End Road, London E1 4NS, United Kingdom

<sup>a)</sup>Current address: Department of Anatomy, Physiology and Biochemistry, Swedish University of Agricultural Sciences, Box 7011, 75007 Uppsala, Sweden.

<sup>b)</sup>Author to whom correspondence should be addressed: [nicola.pugno@unitn.it](mailto:nicola.pugno@unitn.it)

## ABSTRACT

This paper deals with the possibility of merging spider silk with nanomaterials by directly feeding them to the spiders. Indeed, creating a soft “bioncomposite” with enhanced mechanical and/or other multifunctional properties, e.g., electric, magnetic, etc., is attractive for material science. Pugno and co-workers were the first to expose spiders to carbon-based nanomaterials, reporting promising results in terms of silk maximal reinforcements. In a subsequent paper, Kelly and co-workers used a different approach and did not obtain any significant strengthening in the silk. These different results highlight the importance of exploring the issue better. In this work, spiders were exposed to nanomaterial solutions with different protocols, and the properties of their silk were monitored for 14 days, displaying a strong protocol influence and inherent day-to-day variability (up to 300% of a single property). This made this paper’s results aligned with both the previous mentioned works, pinpointing the key challenge to merging silk and nanomaterials using spiders. This work should stimulate further studies and discussion on the topic.

© 2022 Author(s). All article content, except where otherwise noted, is licensed under a Creative Commons Attribution (CC BY) license (<http://creativecommons.org/licenses/by/4.0/>). <https://doi.org/10.1063/5.0095960>

## INTRODUCTION

Spider and silkworm silks are materials with exceptional mechanical and biological properties, and they have been of interest to materials scientists for millennia.<sup>1,2</sup> In particular, silks could be ideal candidates for applications that range from aerospace engineering to biomedical technologies.<sup>3–8</sup>

Nonetheless, silk fibrous’ materials applicability is limited for two reasons. First, to be used as reinforcing material in composites, they should have higher stiffness and strength in order to compete with carbon and glass fibers.<sup>9</sup> Second, although they do possess good mechanical properties, they have poor electromagnetic ones<sup>10</sup> that make them unattractive for soft electronics and robotics applications, e.g., in actuation or sensing.<sup>6,11–13</sup> Moreover, the same is valid

for their applications in biomedical implants that need to introduce electrical stimulation to the target tissue.<sup>14–16</sup> Recently, electrically conducting poly(3,4-ethylene dioxythiophene) polystyrene sulfonate (PEDOT:PSS) has been used to design conductive scaffolds.<sup>17</sup> It is also reported that, when used in the human body environment conditions, PEDOT:PSS can retain 89% of its conductivity, it is easily water processable, but it does not provide structural and mechanical aid.<sup>18</sup>

In this regard, in order to be even more attractive, silk should be merged with materials endowed with both superior mechanical and electrical properties. In this context, carbon-based nanomaterials, and, in particular, graphene and carbon nanotubes, offer an opportunity due to their superlative strength and extreme conductivity.<sup>19</sup> This possibility is supported by the fact that many attempts to

hybridize carbon nanotubes with polymer-based fibers by means of in-spinning protocols (e.g., wet spinning) and post-spinning procedures (e.g., coating) have been reported.<sup>20–24</sup>

In trying to merge silks with carbon-based nanomaterials, silkworm silk has been more investigated with respect to spider silk, since it is produced in large quantities and is easier to process. For example, Zhang *et al.*<sup>25</sup> dry spun regenerated silkworm silk with graphene oxide, obtaining slightly higher Young's modulus and strength for the hybrid fibers, but without an apparent trend related to the concentration of graphene oxide used in the spinning solution. For the carbon nanotubes, electrospinning techniques have been used to produce hybrid silk fibers with discordant results, i.e., in one case, the composite presented worse mechanical properties compared to the control,<sup>26</sup> and in the other case, the mechanical properties were slightly better.<sup>27</sup> A small improvement in the mechanical properties was also obtained by means of wet spinning,<sup>28</sup> but a future related work highlighted that this effect does not follow a specific trend, should be better investigated, and depends strongly on the type of nanomaterial used in the experiments.<sup>29</sup>

Other attempts at merging silkworm silk with nanomaterials consisted of feeding the animals with contaminated food. In particular, it has been shown that spraying the mulberry leaves, on which silkworms feed, with nanomaterial solutions seems to improve the mechanical properties of the outcoming fibers.<sup>30</sup> However, also in this case, the improvement is strongly dependent on the type of nanomaterials used in the solutions and is strongly affected by the inherent variability of the silk as later verified.<sup>31–33</sup>

If merging silkworm silk with nanomaterials is an attractive issue in material science, doing the same with spider silk is even more appealing, given its superior mechanical and biological nature.<sup>34</sup>

In this sense, carbon nanotubes and other nanomaterials have already been used to improve spider silk fiber strength and provide conductivity.<sup>35–38</sup> In the previous cited works, spider silk fibers were treated after their spinning, being exposed to iron–metal vapors or immersed in carbon nanotube solutions. Although these strategies significantly improve the conductivity and the strength of the silk, they generate undesirable side-effects, e.g., excessive water plasticization induced by supercontraction.<sup>39,40</sup> These could be removed by using in-spinning protocols to merge nanomaterials with spider silk. To do so, feeding the animals directly could be an opportunity, as it has been suggested and done, as previously discussed, for silkworm silk.<sup>30</sup>

The idea of feeding spiders with nanomaterials to make them merge with their silk is also supported by the fact that altering the diet of these arachnids may induce changes in the nanostructure of their silk.<sup>41</sup> Moreover, some nutrients offered in the spiders' diet are proved to end up in the final polymeric thread, as it has been recently showed for quinine.<sup>42</sup>

Unfortunately, the digestive system of spiders is very complex and not directly connected with the silk glands.<sup>43</sup> On the other hand, the silkworms spin silk from their mouths to which the silk gland is directly connected, making it easier to contaminate with nanomaterials (Fig. 1). This leads to the fact that finding spider silk contaminated with nanomaterials (if not externally) means that either spiders metabolized them or their glands or spinnerets were contaminated. Furthermore, even if nanomaterials end up in spider silk, they should be in a

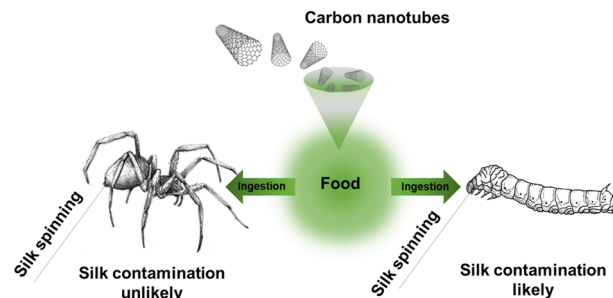


**FIG. 1.** In order to merge spider/silkworm silk and nanotubes, one of the attempts consisted of contaminating the animal food with the nanomaterials. In this case, both silkworms and spiders use the mouth for ingesting food, but the former spin the silk from the very same opening, while the latter from another part of the body. This makes it more difficult to contaminate spider silk with nanomaterials.

sufficiently well incorporated amount to increase the physical properties of the fiber, e.g., strength or conductivity.

In this context, the first attempt to expose spiders to carbon-based nanomaterials has been pioneered by Pugno and co-workers<sup>44,45</sup> (I). This was made by exposing different spider lines to water nanomaterial solutions, by spraying them in the spider terrarium and extracting the silk lines from the webs later produced. A different approach was proposed later by Kelly *et al.*<sup>46</sup> (II) that used nine lines of spiders in which three served as control groups, were fed with nanomaterial solutions, and the silk was forcibly extracted from the animals.

The obtained silk materials studied in (I) and (II) with different approaches led to different results. Indeed, although the presence of nanomaterials in or on the silk was confirmed in (I) through Raman spectroscopy, it was never discussed if the spider silk “composite” was obtained during the spinning by the animals. This was due to the complexity of having a direct proof of the nanomaterials' incorporation into the bulk of the silk during the spinning process. On the other hand, in (II), no nanomaterials were found in the silk. In terms of mechanical properties, the approach (I) reported a significant increase in the silk maximal strength of some spider lines exposed to nanomaterials, especially carbon nanotubes. On the contrary, the approach (II) did not report significant differences in the mechanical properties between the silk of the control lines and those of the lines fed with similar nanomaterials used in (I).

In this work, we discuss this issue by repeating the experiments using approaches similar to those in (I) and (II). In particular, five lines of animals were exposed to different nanotubes and conductive colorant solutions, and their silk was successively extracted every two days for two weeks. This guaranteed the monitoring of the mechanical, structural, and electrical properties for fourteen days. The obtained results are aligned with both works (I) and (II), highlighting the challenges in using these animals to merge silk and nanomaterials because of the inherent biological complexity of spiders and the day-to-day variability of their silk material properties.

## RESULTS AND DISCUSSION

*Steatoda triangulosa* spiders were selected for the study because this species was used in our first paper.<sup>44</sup> Since the mechanical

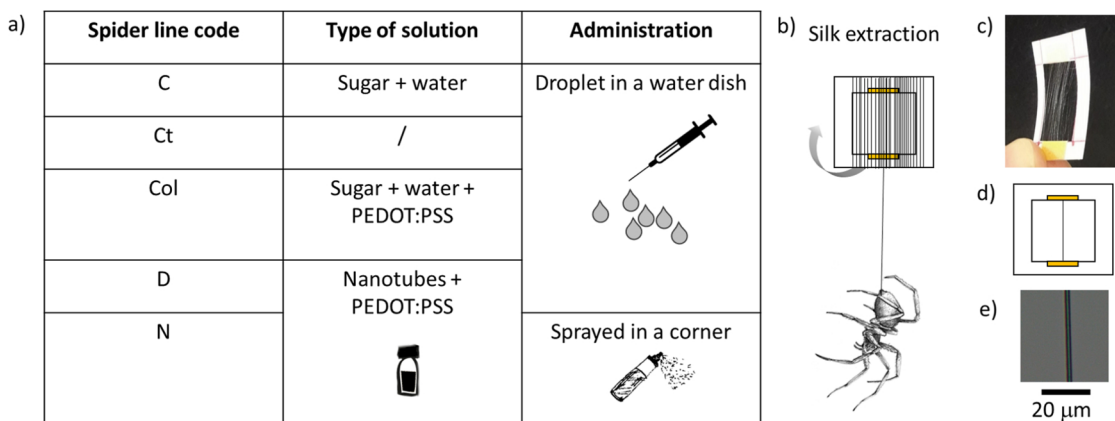


**FIG. 2.** (a) Codes of the analyzed spider lines, types of used solutions, and ways of administration. (b) The silk was forcibly extracted at a speed of about 1 cm/s and collected on (c) a paper frame. (d) Single fibers were extracted from the frame and mounted onto a  $1 \times 1 \text{ cm}^2$  paper frame. (e) The diameters of the fibers were measured by means of light microscopy before the tensile test.

properties of spider silk depend on the species,<sup>47</sup> the results presented here may be different from those of other species. 5 lines of animals were set [Fig. 2(a)] and equally fed with crickets weekly. To have as much similar silk as possible among different animals, these were selected to be of similar weight since the body mass of the spider may affect the mechanical properties of the silk.<sup>48,49</sup> All the solutions that were given to the spiders were sweet (with glucose), since the spiders are attracted by the sweet taste.<sup>50</sup> Among the five lines of animals [Fig. 2(a)], two were used as controls, in which one was not exposed to any solution (the Ct line) and the other one to a glucose–water solution (C line). This was done in order to verify that the sweet solution has no effect on the silk's physical properties. One line of animals was exposed to a sweet solution containing PEDOT:PSS black colored conductive polymer (Col line). This was administered to the animals by means of a water dish set in a corner of the box. The last two lines of animals were used to expose them to carbon nanotube solutions in two different ways: by spraying the solution in a corner, as described in (I)<sup>44</sup> (N line), and the second by watering the spiders with a dish, similarly to what has been done in (II)<sup>46</sup> (D line). The spiders were not forcibly fed, as in,<sup>46</sup> because such a procedure imposed an excessive level of stress that may have affected the mechanical properties of the silk.<sup>51,52</sup> For this reason, here the level of stress was qualitatively judged by taking pictures of the web every two days when each silk extraction was performed (Fig. S1–S5). Overall, the animals did not express any obvious signs of stress despite the fact that N line was exposed to nanomaterials by spraying the solutions in the box.

Spider silk samples were extracted every two days from the animals, which were removed from the boxes and forcibly silked [Fig. 2(b)] at  $\sim 1 \text{ cm/s}$  on a sample holder to obtain bundles of silk [Fig. 2(c)]. From these, single fibers were delicately extracted with forceps, observed with light microscopy to assess their homogeneity, measure their diameters, and finally tensile tested [Figs. 2(d) and 2(e)]. Since the five lines of animals were considered, and these were monitored for 14 days, a total of 35 different sets of fibers were characterized (Fig. S6).

The diameters of the silk fibers analyzed in this study are depicted in Fig. 3. An increase in the diameter with respect to the day has been observed for all the lines with the exception of C line, in which the diameters remained significantly constant during the period. Moreover, for D line on the fourteenth day, a decrease in diameter was detected. On the other hand, considering the same day, no significant differences emerged among the different silk lines. Thus, for a given day, the mechanical properties of the silk fibers can be compared since the diameter of the fibers may affect their mechanical properties.<sup>48</sup>

Carbon nanotubes are considered optimal to reinforce materials, and in this case, a spider silk fiber with enhanced mechanical properties could mean that such nanomaterials were included in the silk. To assess this, tensile tests were performed on the different sets

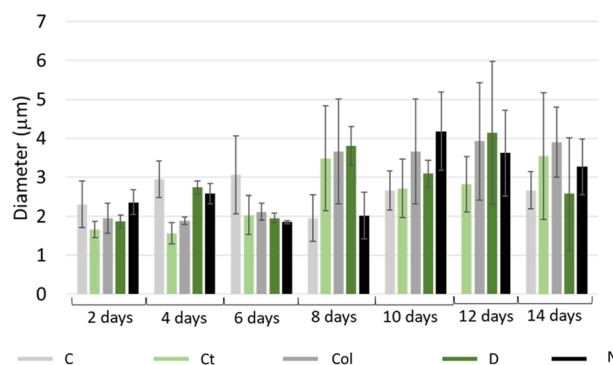


**FIG. 3.** Mean values and standard deviation of the different spider silk fiber diameters at different days. Overall, a slight increase in fiber diameter was observed, but among the groups on the same day, no significant differences were detected.

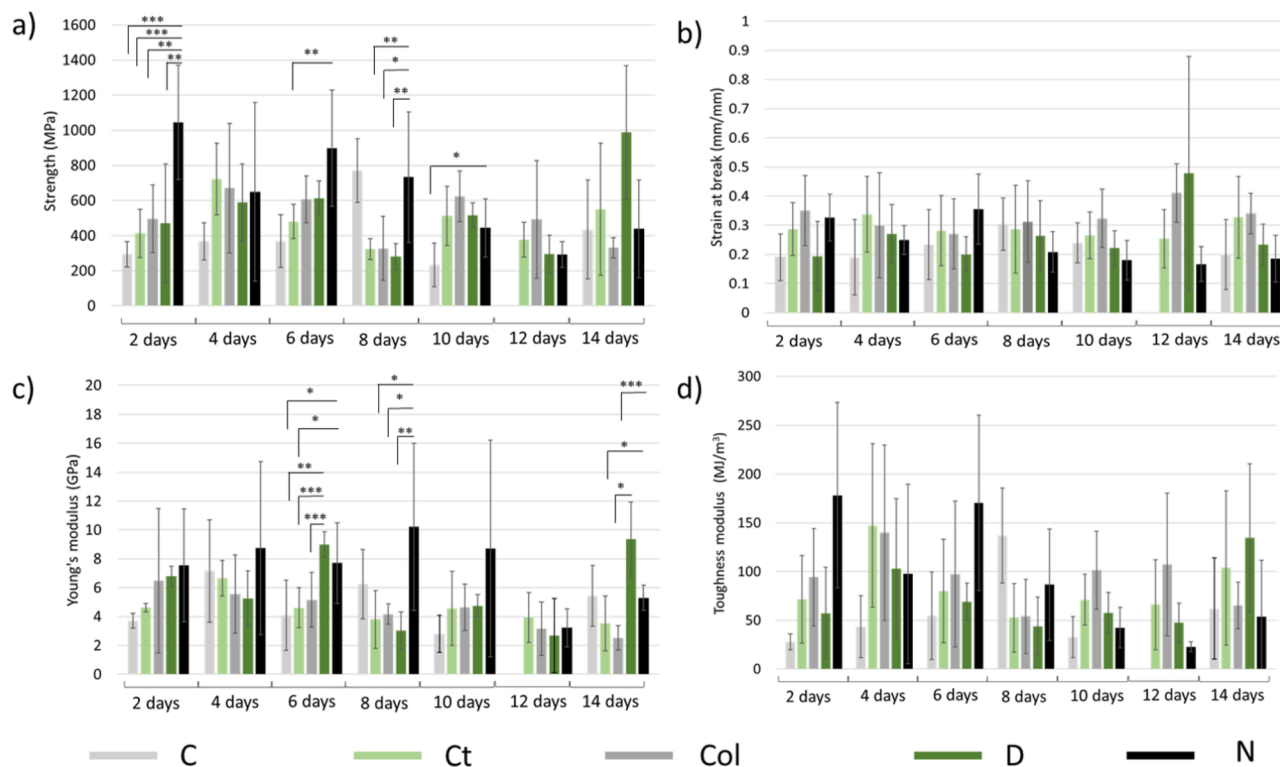


**FIG. 4.** Values of the mechanical properties of the different spider silk fibers at different days: (a) Strength, (b) Strain at break, (c) Young's modulus, and (d) toughness modulus. Stars indicate significant differences and p-values: \* < 0.1, \*\* < 0.05, \*\*\* < 0.01. The data for Col on day 6 are missing because on that day the spider did not spin enough silk. The N and D lines (i.e., the only ones exposed to carbon nanotubes) significantly displayed the highest strengths.

of spider silks, and the results are depicted in Figs. 4(a)–4(d) and S7–S11. Although the mechanical properties of all the silk dataset are highly scattered, which is a natural consequence of silk's inherent variability,<sup>53</sup> some statements can be made. The strength of the silk fibers was not constant during the 14 days [Fig. 4(a)]. In particular, on the second day, N line's strength was significantly the highest (the max strength recorded was nearly 1400 MPa). On the sixth day, the N line had a strength that was significantly higher than the Ct line (the max strength recorded was nearly 1200 MPa), similarly to what was reported in (I)<sup>44</sup> and on the eighth day, the N line had a strength that was higher than the Col, D, and C lines. These had a max strength recorded of nearly 1000, 1300, and 1000 MPa, respectively. Finally, on the tenth day, the N line had a strength that was higher than the Ct line. Despite the D line presenting high strength on the last day, the high scattering made it impossible to assess a significant difference, similarly to what was reported in (II).<sup>46</sup> As expected, the three highest strengths reported were those of D and N lines, i.e., the only ones exposed to carbon nanotube solutions. Moreover, for the N line, a significant decrease in strength was noted with the succession of the day (Fig. S7). This, coupled with the first increase in strength, suggests that the procedure of nebulization could affect positively first and negatively after the mechanical properties of the silk, perhaps due to a higher level of stress in the animal that could increase with time and nanomaterial exposition,

but it is not detectable by simply looking at the spider behavior (Figs. S1–S5).

The strain at break of most of the samples was significantly constant during the 14 days trial [Fig. 4(b)], suggesting that the imposed stress on the animal and the eventual contamination of nanomaterials did not affect such property. This was not true for the N line, in which a slight decrease in strain at break was observed with the successions of the day (Fig. S7). Similar trends were noted for the Young's modulus [Fig. 4(c)]. In particular, on the second and fourth days, no differences were detected. On the sixth day, the D line presented a higher Young's modulus than the Ct, C, and Col lines. At the same time, the N line presented higher values than the Ct and C lines. On the eighth day, the N line presented a higher Young's modulus than the D, Col, and Ct lines; whereas, on the last day, the N line showed higher values with respect to the Col and Ct, and the D had higher values with respect to the Col. For the toughness modulus [Fig. 4(d)], the small increase first and small decrease after with the succession of the day for the N line is in agreement with the previous mentioned trends (a part from the expected larger variability<sup>54</sup>).

Overall, the tensile tests investigation showed that among all the spider lines, the ones exposed to carbon nanotube solutions presented higher strength values compared to the control lines, in agreement with (I).<sup>44</sup> Moreover, with respect to the (II) work,<sup>46</sup> it must be noted that the mechanical properties of the different

spider silks were here monitored for 14 days continuously (with seven time points), in order to gain data from the assumed whole metabolic cycle of the spiders.<sup>55</sup> In this regard, it is important to highlight that because of this day-to-day variability, it may be that two time points, as recorded in,<sup>46</sup> are not enough to detect an eventual modification in the mechanical properties due to the presence of nanotubes, which in any case were not observed here.

To further characterize the fibers, FTIR analysis was conducted to detect the presence of carbon nanotubes and changes in the secondary structure content of the protein (Fig. 5). In this regard, it is possible to notice that the secondary structure content of N line revealed an increase in  $\beta$ -sheet with the succession of the day (a common property associated with fiber's strength<sup>56–58</sup>), despite the strength of this type of fiber decreased. Moreover, the N line presented the lowest amount of  $\beta$ -sheet, despite its strength values being the highest. In this sense, it must be pointed out that a similar trend has recently been found,<sup>59,60</sup> suggesting that the FTIR technique may not be the optimal choice in investigating the secondary structure content of silk microfibrils and the eventual presence of nanomaterials.

In this regard, the measure of silk's electrical properties could help to detect nanomaterials. Indeed, the exposition of living organisms to large quantities of nanomaterials was previously found as a viable method to affect the electrical properties of the so-called "bioncomposites."<sup>61–66</sup> For this reason, even if the nanomaterial quantities are small, conductivity measurements were performed on the spider silk fibers [Fig. 6(a)]. The results are summarized in Figs. 6(b) and 6(c) and S12; in which it is possible to notice

that the values of the conductivity changed day by day considering a single line of animals. Although the data suggest that there is not a clear trend (i.e., the electrical current values are of the same order of magnitude among the different lines), it should be noted that the Col (without carbon nanotubes), D and N lines (with carbon nanotubes) show an asymmetric behavior for negative voltage bias (Fig. S12). In particular, when the negative voltage increased up to  $-6$  V, a gradual increase in current occurred with respect to the value measured at 6 V. Interestingly, this asymmetric behavior was previously observed for PEDOT:PSS, which is one of the most common electrically conducting organic polymers.<sup>67</sup> In addition, the lines exposed to PEDOT:PSS exhibited an insulating property. This might be due to its dilution into the silk fibers. Moreover, the D line showed the lowest resistance values, indicating that these silk fibers were the most naturally conductive. At the same time, the Ct and C lines had the silk with the highest values of resistance. Thus, the conductivity experiments provided insights on the presence of nanomaterials in the silk and pointed out the need for further investigation into the synergy between nanomaterials and their carrier. Finally, as discussed previously, the presence of carbon nanotubes inside the silk is not solely sufficient to improve the conductivity of the composite.<sup>20–23</sup> The information on changes in the secondary structure content (i.e., turns structure) recorded on the D composite could reveal the mechanisms of the change in the electric behavior (Fig. 6) due to a synergistic effect of PEDOT:PSS and carbon nanotubes elucidated by Pan *et al.*<sup>35</sup> They proposed by dissipative particle dynamic simulation that the hydrogen bond in the amorphous structure was broken with strain increasing and that the

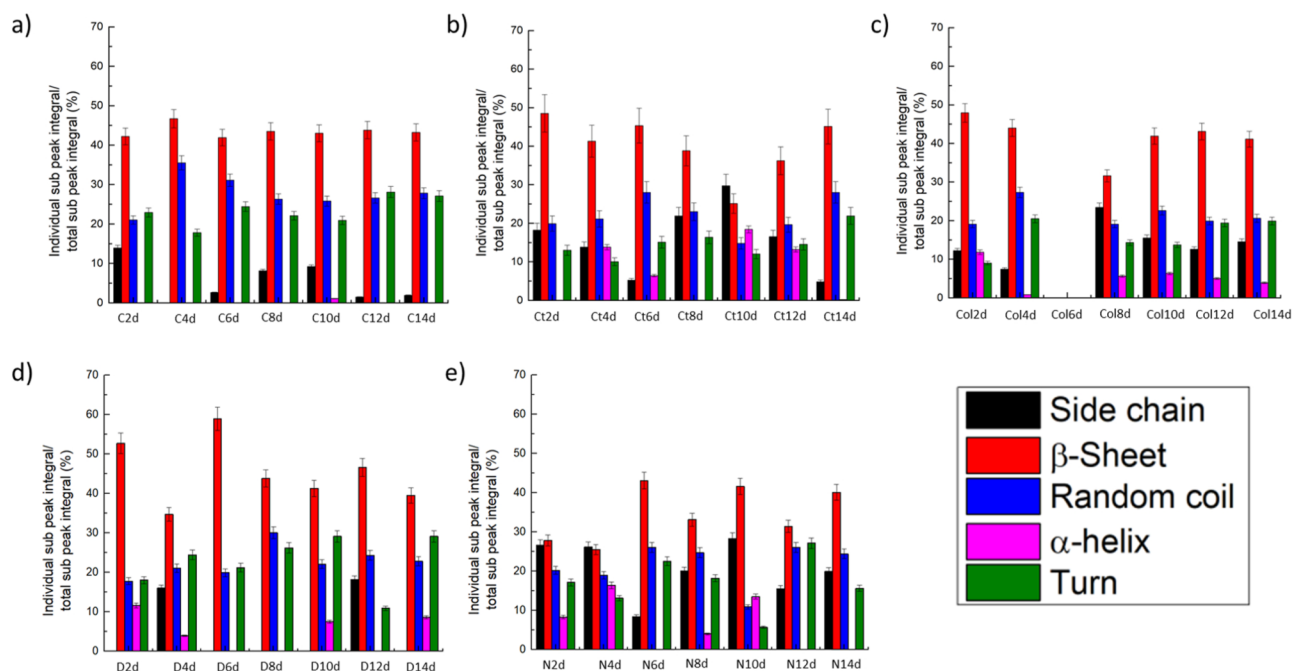


**FIG. 5.** Secondary content of the different spider silk types obtained by means of FTIR spectroscopy for the (a) C samples, (b) Ct samples, (c) Col samples, (d) D samples, and (e) N samples. The data for Col6d are missing because on that day the spider did not spin enough silk.

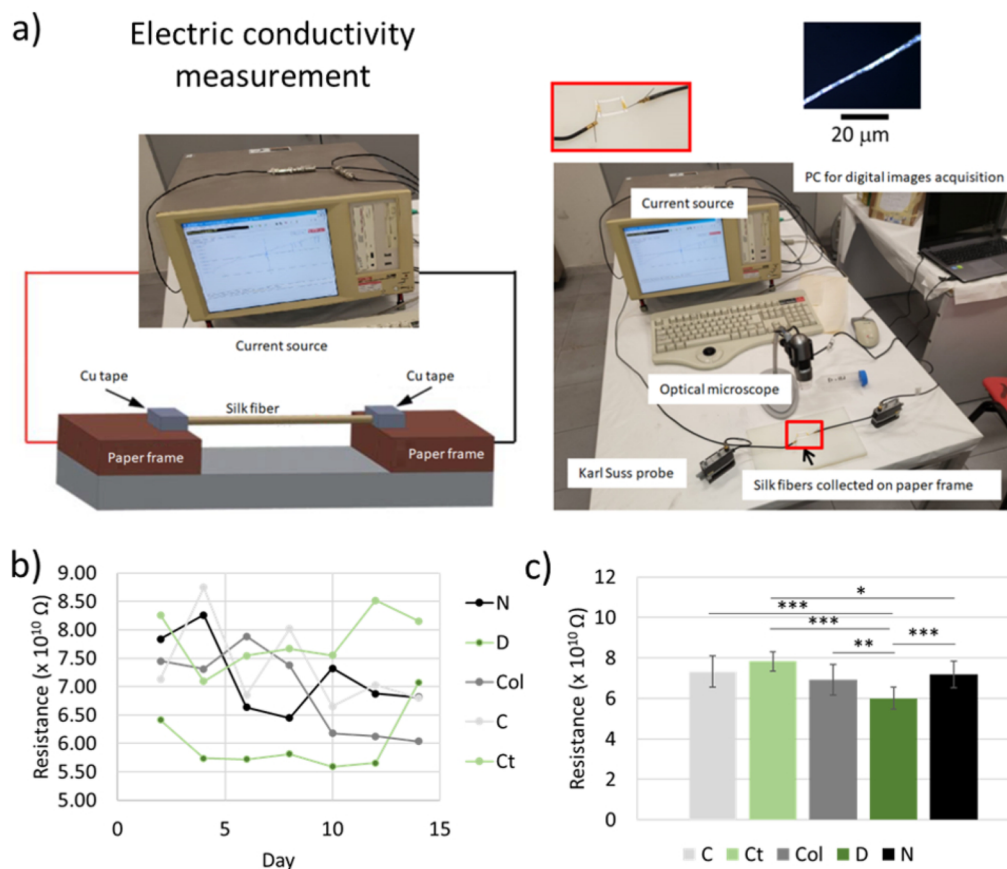


**FIG. 6.** (a) Schematic of the experimental principle and setup provided for the electrical measurements. The red square in the zoom indicates the fibers collected on the paper frame. An image of the single fiber recorded by means of light microscopy. (b) Values of the resistances of the silk fibers measured on different days and (c) mean values of the resistances of the silk fibers for different lines of spiders. Stars indicate significant differences and p-values: \* < 0.1, \*\* < 0.05, \*\*\* < 0.01.

interactions between the nanotube and silk protein induced higher conductivity.

## CONCLUSIONS

In general, contrary to what happens for the silkworms, it is quite evident that merging silk with nanomaterials using the spider model poses great challenges since the spider silk properties show large day-to-day variability even in the control lines. Despite this, the obtained results seem to confirm the reinforcing effects of nanomaterials when they are sprayed in the terrarium [in agreement with (I)]. On the other hand, in the other protocols it was not possible to pinpoint trends in the mechanical properties of silk and understand the eventual effect of carbon nanotubes [in agreement with (II)].

By monitoring for the first time the physical properties of the different protocols of silk for fourteen days, the key challenge to merge silk and nanomaterials using spiders has been pinpointed. This work is thus aimed to stimulate further study and discussion on this emerging field of bioncomposites, merging spider silk with nanomaterials, also using more scalable models, such as artificial silk, as we are also investigating.

## MATERIALS AND METHODS

### Spiders

The spiders used in the study were female specimens (0.03–0.13 gr) of *Steatoda triangulosa*, which were farmed in plastic terrariums, watered and fed weekly with water droplets and crickets, respectively. All the animals were kept at room temperature (19–21 °C) and fed weekly with crickets farmed in the lab. Every two days, the animals were removed from the cage, forcibly silked (described below), and then moved again into their cage. Every two days we took a picture of the cage to check if the web showed clear marks of animal stress and possible mold due to the spraying of carbon nanotube solutions. No spiders died after the treatment, and all of them are currently alive and healthy.

### Administration of different solutions

To expose the spiders to different solutions, we designed five spider lines: C, Ct, Col, D, and N. In the control line (C), the animals were kept without being exposed to any substances. In the Ct

line, the spiders were watered (with a water dish) with a sweet solution made of sugar and water. Spiders are known to be attracted to sweet solutions.<sup>55</sup> In the Col line, the spiders were watered (with a water dish) with a sweet solution made of sugar and a conductive polymer (described below). In the D line, the spiders were watered (with a water dish) with a sweet solution made of carbon nanotubes and sugar (as described below). In the last line (N), the spiders were exposed to the previous nanomaterial sweet solution by means of nebulization, which was performed in a corner of the animals' enclosure.

### Silk extraction and tensile tests

As previously mentioned, the spiders were removed from the cage every two days. Then they were silked on a paper support with a reeling speed of  $\sim 1$  cm/s. In this way, on the paper support, there was a bundle of silk fibers. From this, single fibers were carefully extracted with forceps and mounted (glued) on a  $1 \times 1$  cm<sup>2</sup> paper frame with the support of a double-sided tape. To check that single fibers were mounted, for each sample an optical microscopy picture was taken. In this way, the gauge length of the single fiber was about 1 cm.

Then, the diameter was measured in five points and then averaged, with the support of this optical microscopy picture by means of ImageJ.<sup>68</sup> Then, the fiber samples were mounted on a nanotensile Agilent Technology UTM T150 machine and tensile tested. The strain rate was 1% gauge length per second ( $\sim 6$  mm/min). The declared sensitivity of the machine is 1 nN for the load and 0.1 nm for the displacement. From the load displacement curves, the engineering stress was calculated by dividing the load by the initial cross-sectional area of the fiber and the engineering strain was calculated by dividing the displacement by the gauge length. The Young's modulus of the fibers was calculated as the slope of the fitting line in the initial elastic region of the stress strain curve, and the toughness modulus as the area under the stress strain curve. For each dataset, 35 in total, at least five samples were tested. The mechanical properties of the spider's line silk were, thus, monitored for 14 days, which corresponds to the measured metabolism cycle for several species of spiders.<sup>55,69</sup>

### FTIR spectroscopy

FTIR investigations were carried out on the spider silk fibers using a PerkinElmer spectrometer in transmission mode. Measurements were performed in the range of 4000 to 400 cm<sup>-1</sup> with a resolution of 4 cm<sup>-1</sup> and the number of scans was 200 for each spectrum. The background spectra were recorded before each spectrum. The measurements were performed at room temperature. The spectra were collected in the range of 1720 to 1590 cm<sup>-1</sup>, which is the amide I band. The spectra were then deconvoluted by subtracting a linear baseline and applying a Gaussian deconvoluting curve by Origin 9 software. The secondary protein structure content was determined by fitting peaks that were assigned<sup>70-74</sup> with side chains (1605–1616 cm<sup>-1</sup>),  $\beta$ -sheets (1616–1622, 1622–1628, 1628–1638, and 1697–1704 cm<sup>-1</sup>), random coils (1638–1647 and 1647–1656 cm<sup>-1</sup>),  $\alpha$ -helices (1656–1663 cm<sup>-1</sup>), and turns (1663–1671, 1671–1686, and 1686–1697 cm<sup>-1</sup>). The quantification

of the secondary structure proportions was determined by the ratio of the respective sub-peak integrals to the total sub-peak integral.

### Conductive polymer and nanotubes solutions

PEDOT:PSS (poly(3,4-ethylenedioxythiophene):poly(styrene-sulfonate)) 1.3% dispersion in water, conductive grade and CNT water solution (carbon nanotubes single-walled, conductive aqueous ink, SWCNT 0.2 mg/ml dispersed in water with SDS, electrical conductivity  $< 400$   $\Omega$ /sq (by four-point probe on prepared film by spray), 10–20 nm diameter) were supplied by Merck Italy. The PEDOT:PSS/sugar solution (PEDOT:PSS 50 ml, glucose 2.5 g, water 80 ml) was prepared according to the following procedure: glucose was previously dissolved in water and mixed with the PEDOT:PSS water solution using magnetic stirring for 5 min at room temperature. The CNT/PEDOT:PSS/sugar solution (PEDOT:PSS 40 ml, CNT water solution 10 ml, glucose 2.5 g, water 80 ml) was prepared with the same procedure by replacing 10 ml of PEDOT:PSS solution with the same quantity of CNT water solution.

### Electrical characterization

The electrical characterization was performed on the paper frame, where a bundle of silk fibers was collected. Optical microscopy was used to select a single fiber and for the positioning of the Cu tape at the two ends of the fiber. The electrical measurements were then performed by cutting the two lateral sides of the paper frame and using a two-probe system; the probes used, Karl Suss PH100 probe heads, were connected to a PC driven Keithley 4200 SCS. The current–voltage (*I*–*V*) characteristic of each fiber was finally measured at room temperature.

### SUPPLEMENTARY MATERIAL

See the [supplementary material](#) for the pictures of the terrariums of the spiders during the experiments, the sample coding, all the mechanical properties points, and the current voltage curves related to electrical conductivity experiments.

### ACKNOWLEDGMENTS

G.G. would like to thank the following students for their help in the experimental activity: Marianna Gaggiano, Camilla Piva, Chiara Cogotti, Flavia Coluccia, and Erica Bortolameotti. N.M.P. is supported by the Italian Ministry of Education, University and Research (MIUR), under the PRIN-2017TTP3S Grants. G.G. was supported by Caritro Foundation (Grant No. prot. U1277.2020/SG.1130). L.V. received funding from the Italian Ministry of Education, University and Research (MIUR), under the PRIN Project Grant No. 2017FWC3WC. L.V. would like to thank Dr. Silvia Bittolo Bon for her help in the diet preparation. Ref. 44 was published in Arxiv in 2015.<sup>45</sup>

### AUTHOR DECLARATIONS

#### Conflict of Interest

The authors have no conflicts to disclose.



## Author Contributions

**Gabriele Greco:** Data curation (lead); Investigation (equal); Methodology (equal); Writing – original draft (lead); Writing – review & editing (equal). **Luca Valentini:** Data curation (equal); Investigation (equal); Methodology (equal); Writing – review & editing (equal). **Nicola M. Pugno:** Conceptualization (equal); Funding acquisition (equal); Supervision (equal).

## DATA AVAILABILITY

The data that support the findings of this study are available within the article and its [supplementary material](#).

## REFERENCES

- C. Holland, K. Numata, J. Rnjak-Kovacina, and F. P. Seib, “The biomedical use of silk: Past, present, future,” *Adv. Healthcare Mater.* **8**, e1800465 (2019).
- G. Greco and N. M. Pugno, “Mechanical properties and weibull scaling laws of unknown spider silks,” *Molecules* **25**, 2938 (2020).
- B. Xu, Y. Yang, Y. Yan, and B. Zhang, “Bionics design and dynamics analysis of space webs based on spider predation,” *Acta Astronaut.* **159**, 294–307 (2019).
- G. H. Altman *et al.*, “Silk-based biomaterials,” *Biomaterials* **24**, 401–416 (2003).
- S. Salehi, K. Koeck, and T. Scheibel, “Spider silk for tissue engineering applications,” *Molecules* **25**, 737 (2020).
- C. Wang, K. Xia, Y. Zhang, and D. L. Kaplan, “Silk-based advanced materials for soft electronics,” *Acc. Chem. Res.* **52**, 2916 (2019).
- F. G. Omenetto and D. L. Kaplan, “New opportunities for an ancient material,” *Science* **329**, 528–531 (2010).
- A. Dellaquila *et al.*, “Optimized production of a high-performance hybrid biomaterial: Biomaterialized spider silk for bone tissue engineering,” *J. Appl. Polym. Sci.* **10**, 48739 (2019).
- D. U. Shah, D. Porter, and F. Vollrath, “Can silk become an effective reinforcing fibre? A property comparison with flax and glass reinforced composites,” *Compos. Sci. Technol.* **101**, 173–183 (2014).
- S. K. Karan *et al.*, “Nature driven spider silk as high energy conversion efficient bio-piezoelectric nanogenerator,” *Nano Energy* **49**, 655–666 (2018).
- B. D. Gates, “Flexible electronics,” *Science* **323**, 1566–1567 (2009).
- J. Xiong, J. Chen, and P. S. Lee, “Functional fibers and fabrics for soft robotics, wearables, and human–robot interface,” *Adv. Mater.* **33**, e2002640 (2020).
- F. Spizzo, G. Greco, L. Del Bianco, M. Coisson, and N. M. Pugno, “Magnetostrictive and electroconductive stress-sensitive functional spider silk,” *Adv. Funct. Mater.* **1–14**, 2207382 (2022).
- S. Khorshidi and A. Karkhaneh, “Formation of three-dimensionality in polyaniline-based nanofibers: A highly conductive permeable scaffold for stem cells residence,” *Int. J. Polym. Mater. Polym. Biomater.* **65**, 629–635 (2016).
- B. Jakubiec *et al.*, “In vitro cellular response to polypyrrole-coated woven polyester fabrics: Potential benefits of electrical conductivity,” *J. Biomed. Mater. Res.* **41**, 519–526 (1998).
- K. M. Molapo *et al.*, “Electronics of conjugated polymers (I): Polyaniline,” *Int. J. Electrochem. Sci* **7**, 11859–11875 (2012).
- M. Hesam Mahmoudinezhad, A. Karkhaneh, and K. Jadidi, “Effect of PEDOT:PSS in tissue engineering composite scaffold on improvement and maintenance of endothelial cell function,” *J. Biosci.* **43**, 307–319 (2018).
- H. Yamato, M. Ohwa, and W. Wernet, “Stability of polypyrrole and poly(3, 4-ethylenedioxythiophene) for biosensor application,” *J. Electroanal. Chem.* **397**, 163–170 (1995).
- Y. Bai *et al.*, “Carbon nanotube bundles with tensile strength over 80 GPa,” *Nat. Nanotechnol.* **13**, 589 (2018).
- I. A. Kinloch, J. Suhr, J. Lou, R. J. Young, and P. M. Ajayan, “Composites with carbon nanotubes and graphene: An outlook,” *Science* **362**, 547–553 (2018).
- S. Goutianos and T. Peijs, “On the low reinforcing efficiency of carbon nanotubes in high-performance polymer fibres,” *Nanocomposites* **7**, 53–69 (2021).
- A. Mikhilchian and J. J. Vilatela, “A perspective on high-performance CNT fibres for structural composites,” *Carbon* **150**, 191–215 (2019).
- A. Takakura *et al.*, “Strength of carbon nanotubes depends on their chemical structure,” *Nat. Commun.* **10**, 3040 (2019).
- Y. Wang *et al.*, “Design, fabrication, and function of silk-based nanomaterials,” *Adv. Funct. Mater.* **28**, 1–24 (2018).
- C. Zhang, Y. Zhang, H. Shao, and X. Hu, “Hybrid silk fibers dry-spun from regenerated silk fibroin/graphene oxide aqueous solutions,” *ACS Appl. Mater. Interfaces* **8**, 3349–3358 (2016).
- J. Ayutsede *et al.*, “Carbon nanotube reinforced *Bombyx mori* silk nanofibers by the electrospinning process,” *Biomacromolecules* **7**, 208–214 (2006).
- H. Pan *et al.*, “Significantly reinforced composite fibers electrospun from silk fibroin/carbon nanotube aqueous solutions,” *Biomacromolecules* **13**, 2858 (2012).
- G. Fang *et al.*, “Tough protein–carbon nanotube hybrid fibers comparable to natural spider silks,” *J. Mater. Chem. B* **3**, 3940–3947 (2015).
- Z. Yin *et al.*, “Biomimetic mechanically enhanced carbon nanotube fibers by silk fibroin infiltration,” *Small* **17**, 2100066 (2021).
- J.-T. Wang *et al.*, “Directly obtaining high strength silk fiber from silkworm by feeding carbon nanotubes,” *Mater. Sci. Eng. C* **34**, 417–421 (2014).
- Q. Wang, C. Wang, M. Zhang, M. Jian, and Y. Zhang, “Feeding single-walled carbon nanotubes or graphene to silkworms for reinforced silk fibers,” *Nano Lett.* **16**, 6695–6700 (2016).
- N. Ramos *et al.*, “Toward spinning greener advanced silk fibers by feeding silkworms with nanomaterials,” *ACS Sustainable Chem. Eng.* **8**, 011872 (2020).
- H. Xu, W. Yi, D. Li, P. Zhang, S. Yoo, L. Bai, J. Hou, and X. Hou, “Obtaining high mechanical performance silk fibers by feeding purified carbon nanotube/lignosulfonate composite to silkworms,” *RSC Adv.* **9**, 3558–3569 (2019).
- L. Cheng, J. Shao, F. Wang, Z. Li, and F. Dai, “Strain rate dependent mechanical behavior of *B. mori* silk, *A. assama* silk, *A. pernyi* silk and *A. ventricosus* spider silk,” *Mater. Des.* **195**, 108988 (2020).
- L. Pan *et al.*, “A supertough electro-tendon based on spider silk composites,” *Nat. Commun.* **11**, 1332 (2020).
- E. Steven *et al.*, “Carbon nanotubes on a spider silk scaffold,” *Nat. Commun.* **4**, 2435 (2013).
- E. L. Mayes, F. Vollrath, and S. Mann, “Fabrication of magnetic spider silk and other silk-fiber composites using inorganic nanoparticles,” *Adv. Mater.* **10**, 801–805 (1998).
- S.-M. Lee *et al.*, “Greatly increased toughness of infiltrated spider silk,” *Science* **324**, 488–492 (2009).
- Y. Liu, Z. Shao, and F. Vollrath, “Relationships between supercontraction and mechanical properties of spider silk,” *Nat. Mater.* **4**, 901–905 (2005).
- M. Elices, G. R. Plaza, J. Pérez-Rigueiro, and G. V. Guinea, “The hidden link between supercontraction and mechanical behavior of spider silks,” *J. Mech. Behav. Biomed. Mater.* **4**, 658–669 (2011).
- S. J. Blamires, M. Nobbs, J. O. Wolff, and C. Heu, “Nutritionally induced nanoscale variations in spider silk structural and mechanical properties,” *J. Mech. Behav. Biomed. Mater.* **125**, 104873 (2022).
- D. Mebs, C. Wunder, and S. W. Toennes, “Coping with noxious effects of quinine by praying mantids (Mantodea) and spiders (Araneae),” *Toxicol.* **162**, 57–60 (2019).
- R. F. Foelix, *Biology of Spiders* (Oxford University Press, 2011).
- E. Lepore *et al.*, “Spider silk reinforced by graphene or carbon nanotubes,” *2D Mater.* **4**(3), 031013 (2015).
- E. Lepore *et al.*, “Silk reinforced with graphene or carbon nanotubes spun by spiders,” *Arxiv:10.48550/arXiv.1504.06751* (2015).
- S. P. Kelly *et al.*, “Mechanical and structural properties of major ampullate silk from spiders fed carbon nanomaterials,” *PLoS One* **15**, 02418299 (2020).
- I. Agnarsson, M. Kuntner, and T. A. Blackledge, “Bioprospecting finds the toughest biological material: Extraordinary silk from a giant riverine orb spider,” *PLoS One* **5**, e11234 (2010).

- <sup>48</sup>A. T. Sensenig, I. Agnarsson, and T. A. Blackledge, "Adult spiders use tougher silk: Ontogenetic changes in web architecture and silk biomechanics in the orb-weaver spider," *J. Zool.* **285**, 28–38 (2011).
- <sup>49</sup>D. Piorkowski, C.-P. Liao, T. A. Blackledge, and I.-M. Tso, "Size-related increase in inducible mechanical variability of major ampullate silk in a huntsman spider (Araneae: Sparassidae)," *Sci. Nat.* **108**, 22 (2021).
- <sup>50</sup>C. Viera and M. O. Gonzaga, *Behaviour and Ecology of Spiders* (Springer, 2017).
- <sup>51</sup>C. S. Ortlepp and J. M. Gosline, "Consequences of forced silking," *Biomacromolecules* **5**, 727–731 (2004).
- <sup>52</sup>J. Pérez-Rigueiro, "The effect of spinning forces on spider silk properties," *J. Exp. Biol.* **208**, 2633–2639 (2005).
- <sup>53</sup>G. Greco, H. Mirbaha, B. Schmuck, A. Rising, and N. M. Pugno, "Artificial and natural silk materials have high mechanical property variability regardless of sample size," *Sci. Rep.* **12**, 3509 (2022).
- <sup>54</sup>J. R. Taylor, *Introduction to Errors Analysis: The Study of Uncertainties in Physical Measurements* (University Science Books, 1997).
- <sup>55</sup>R. Foelix, *Biology of Spider* (Oxford University Press, 2011), Vol. 53.
- <sup>56</sup>P. Papadopoulos, J. Sölter, and F. Kremer, "Structure-property relationships in major ampullate spider silk as deduced from polarized FTIR spectroscopy," *Eur. Phys. J. E* **24**, 193–199 (2007).
- <sup>57</sup>F. Vollrath, "Strength and structure of spiders' silks," *Rev. Mol. Biotechnol.* **74**, 67–83 (2000).
- <sup>58</sup>T. Asakura and T. Miller, *Biotechnology of Silk* (Springer Dordrecht, 2014), Vol. 5.
- <sup>59</sup>H. Zhu *et al.*, "Tensile properties of synthetic pyriform spider silk fibers depend on the number of repetitive units as well as the presence of N- and C- terminal domain," *Int. J. Biol. Macromol.* **154**, 765 (2020).
- <sup>60</sup>K. Z. Htut *et al.*, "Correlation between protein secondary structure and mechanical performance for the ultra-tough dragline silk of Darwin's bark spider," *J. R. Soc. Interface* **18**, 20210320 (2021).
- <sup>61</sup>L. Valentini, S. Bittolo Bon, S. Signetti, and N. M. Pugno, "Graphene-based bionic composites with multifunctional and repairing properties," *ACS Appl. Mater. Interfaces* **8**, 7607–7612 (2016).
- <sup>62</sup>L. Valentini *et al.*, "Fermentation based carbon nanotube multifunctional bionic composites," *Sci. Rep.* **6**, 27031 (2016).
- <sup>63</sup>L. Valentini, S. B. Bon, and N. M. Pugno, "Microorganism nutrition processes as a general route for the preparation of bionic nanocomposites based on intractable polymers," *ACS Appl. Mater. Interfaces* **8**, 22714–22720 (2016).
- <sup>64</sup>N. M. Pugno and L. Valentini, "Bionic composites," *Nanoscale* **11**, 3102 (2019).
- <sup>65</sup>L. Valentini, S. Bittolo Bon, and N. Pugno, "Combining living microorganisms with regenerated silk provides nanofibril-based thin films with heat-responsive wrinkled states for smart food packaging," *Nanomaterials* **8**, 518 (2018).
- <sup>66</sup>L. Valentini, S. B. Bon, and N. M. Pugno, "Graphene and carbon nanotubes auxetic rubber bionic composites, with negative variation of the electrical resistance and comparison with their non-bionic counterparts," *Adv. Funct. Mater.* **27**, 1606526 (2017).
- <sup>67</sup>S. Kirchmeyer and K. Reuter, "Scientific importance, properties and growing applications of poly(3,4-ethylenedioxythiophene)," *J. Mater. Chem.* **15**, 2077–2088 (2005).
- <sup>68</sup>C. A. Schneider, W. S. Rasband, and K. W. Eliceiri, "NIH image to ImageJ: 25 years of image analysis," *Nat. Methods* **9**, 671–675 (2012).
- <sup>69</sup>W. Nentwig, *Spider Ecophysiology* (Springer Berlin, Heidelberg, 2013).
- <sup>70</sup>X. Hu, D. Kaplan, and P. Cebe, "Determining beta-sheet crystallinity in fibrous proteins by thermal analysis and infrared spectroscopy," *Macromolecules* **39**, 6161–6170 (2006).
- <sup>71</sup>J. Petzold *et al.*, "Surface features of recombinant spider silk protein eADF4 ( $\kappa$ 16)-made materials are well-suited for cardiac tissue engineering," *Adv. Funct. Mater.* **27**, 1701427 (2017).
- <sup>72</sup>C. B. Borkner, S. Lentz, M. Müller, A. Fery, and T. Scheibel, "Ultra-thin spider silk films: Insights into spider silk assembly on surfaces," *ACS Appl. Polymer Mater.* **1**, 3366 (2019).
- <sup>73</sup>C. Thamm and T. Scheibel, "Recombinant production, characterization, and fiber spinning of an engineered short major ampullate spidroin (MaSp1s)," *Biomacromolecules* **18**, 1365–1372 (2017).
- <sup>74</sup>E. DeSimone, T. B. Aigner, M. Humenik, G. Lang, and T. Scheibel, "Aqueous electrospinning of recombinant spider silk proteins," *Mater. Sci. Eng. C* **106**, 110145 (2020).

1 **Supplementary Material**

2 Advances in the use of spiders for direct spinning of nano-reinforced silk

3

4 Gabriele Greco<sup>1,+</sup>, Luca Valentini<sup>2</sup> and Nicola M. Pugno<sup>1,3\*</sup>

5

6 <sup>1</sup> Laboratory for Bioinspired, Bionic, Nano, Meta, Materials & Mechanics, Department of Civil,  
7 Environmental and Mechanical Engineering, University of Trento, Via Mesiano, 77, 38123 Trento,  
8 Italy

9 <sup>2</sup> Department of Civil and Environmental Engineering, University of Perugia and INSTM Research  
10 Unit, Strada di Pentima 4, 05100 Terni, Italy

11 <sup>3</sup> School of Engineering and Materials Science, Queen Mary University of London, Mile End Road,  
12 London E1 4NS, UK

13

14 \* Corresponding author: [nicola.pugno@unitn.it](mailto:nicola.pugno@unitn.it);

15 + currently at Department of Anatomy, Physiology and Biochemistry, Swedish University of  
16 Agricultural Sciences, Box 7011, 75007 Uppsala, Sweden

17

18 **Keywords:** bionicomposites; mechanical properties; tensile tests; carbon nanotubes;  
19 nanomaterials; spider silk;

20

21 In this supplementary material are the pictures of the terrarium of the spiders during the  
22 experiments, the samples coding, all the mechanical properties points, and the current voltage  
23 curves related to electrical conductivity experiments.

24



25

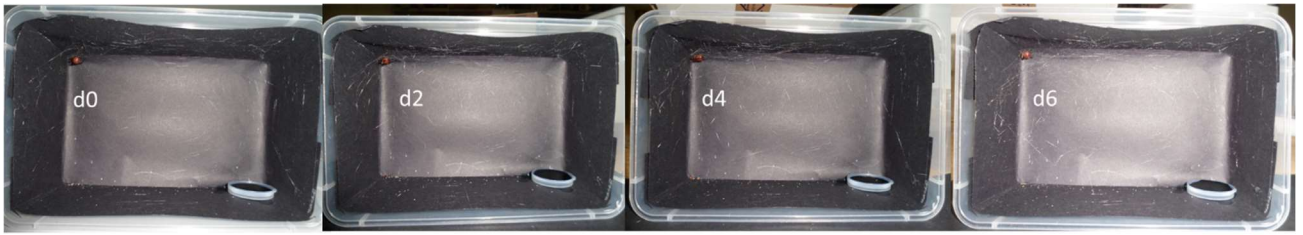
26 *Figure S1: Pictures of the cage in which N line spiders was kept and exposed to carbon nanotube solutions.*

27

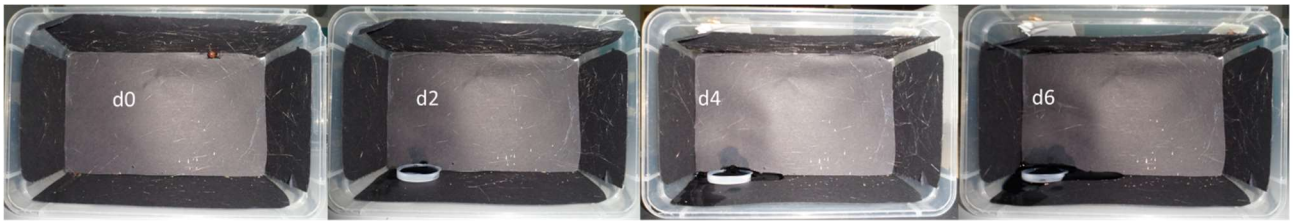
28

29

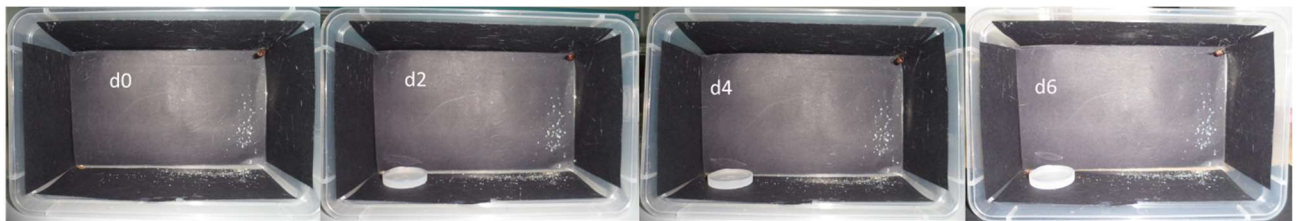
30



31  
32 *Figure S2: Pictures of the cage in which D line spiders was kept and exposed to carbon nanotube solutions.*



33  
34 *Figure S3: Pictures of the cage in which Col line spiders was kept and exposed to carbon nanotube solutions.*



35  
36 *Figure S4: Pictures of the cage in which C line spiders was kept and exposed to carbon nanotube solutions.*



37

38 *Figure S5: Pictures of the cage in which Ct line spiders was kept and exposed to carbon nanotube solutions.*

39

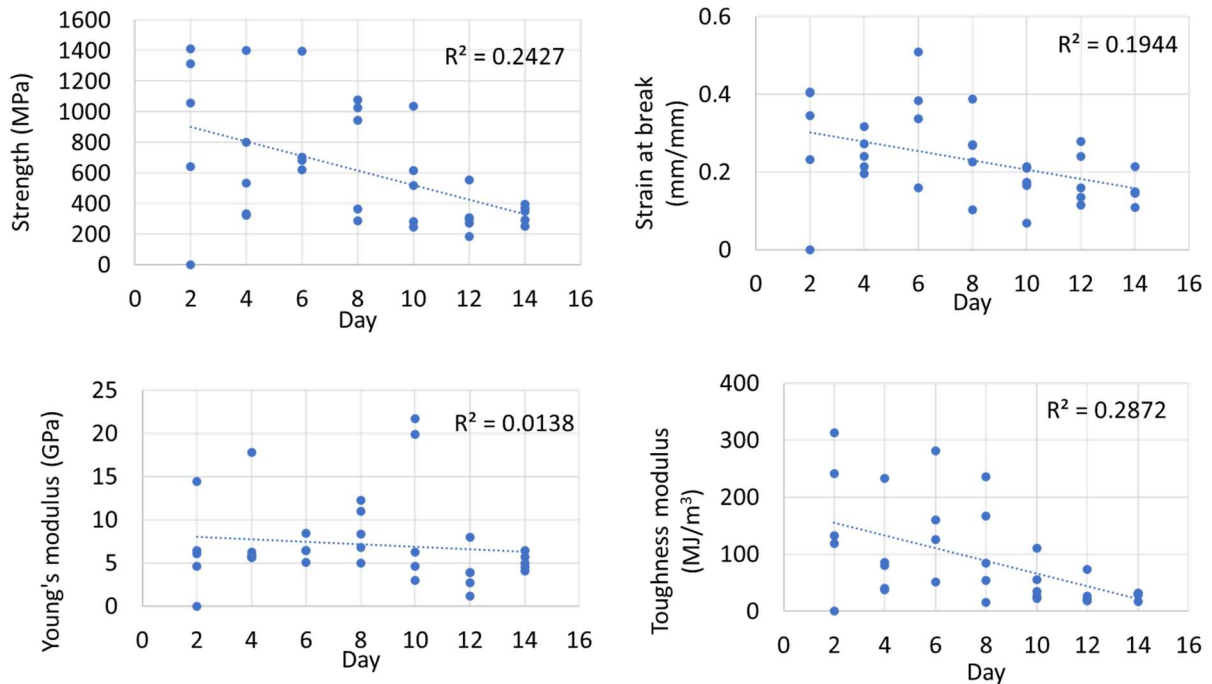
Time point	Control (nothing)	Control (sweet solution)	Coloured (colourant solution)	Nanomaterials	
				Droplet (Solution)	Nebulization (Solution)
2 days (2d)	Ct – 2d	C – 2d	Col – 2d	D – 2d	N – 2d
4 days (4d)	Ct – 4d	C – 4d	Col – 4d	D – 4d	N – 4d
6 days (6d)	Ct – 6d	C – 6d	Col – 6d	D – 6d	N – 6d
8 days (8d)	Ct – 8d	C – 8d	Col – 8d	D – 8d	N – 8d
10 days (10d)	Ct – 10d	C – 10d	Col – 10d	D – 10d	N - 10d
12 days (12 d)	Ct – 12 d	C – 12 d	Col – 12d	D – 12d	N – 12d
14 days (14d)	Ct – 14 d	C – 14 d	Col – 14d	D – 14d	N – 14d

40

41 *Figure S6: All the different codes for the samples of spider silk that were analyzed in this study.*

42

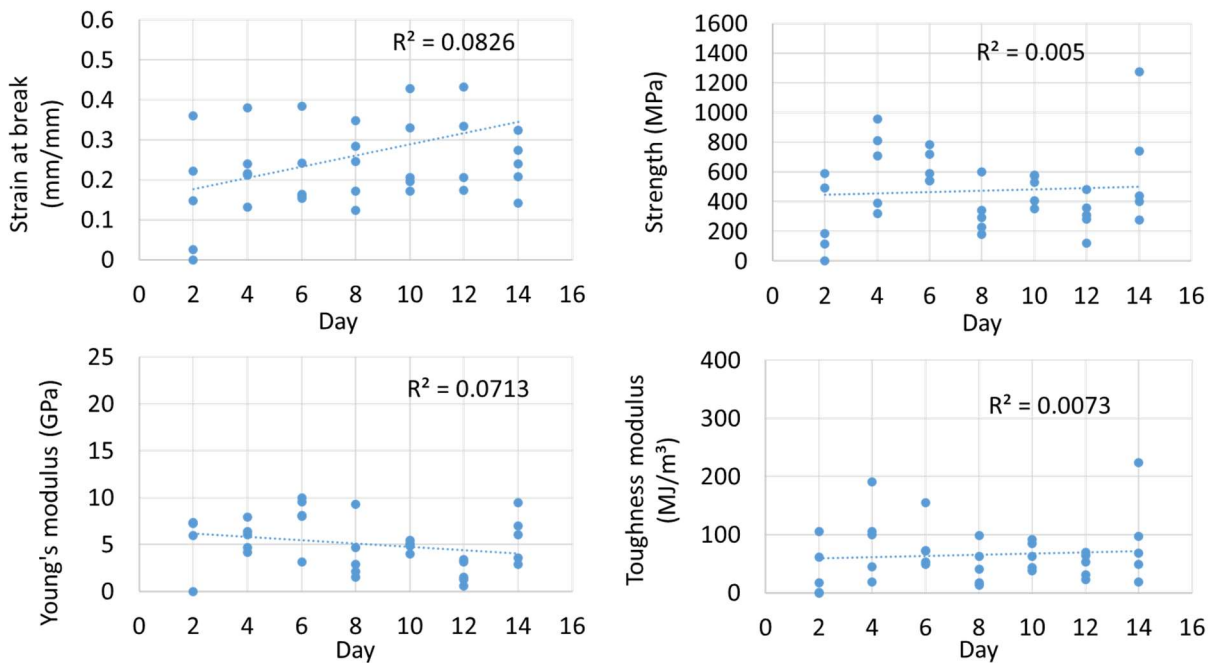
## N samples



43  
44

Figure S7: All the mechanical properties of the N line of spider silk. The dashed line represents the trend with its relative  $R^2$  value.

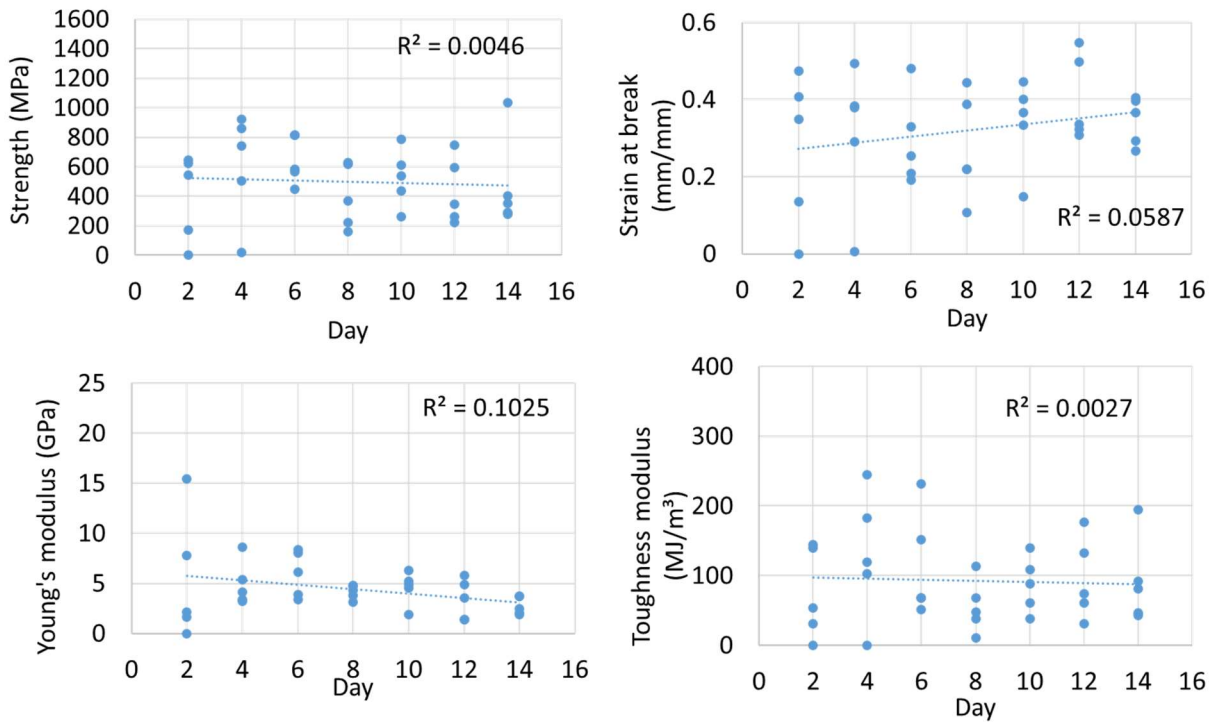
## D samples



45  
46

Figure S8: All the mechanical properties of the D line of spider silk. The dashed line represents the trend with its relative  $R^2$  value.

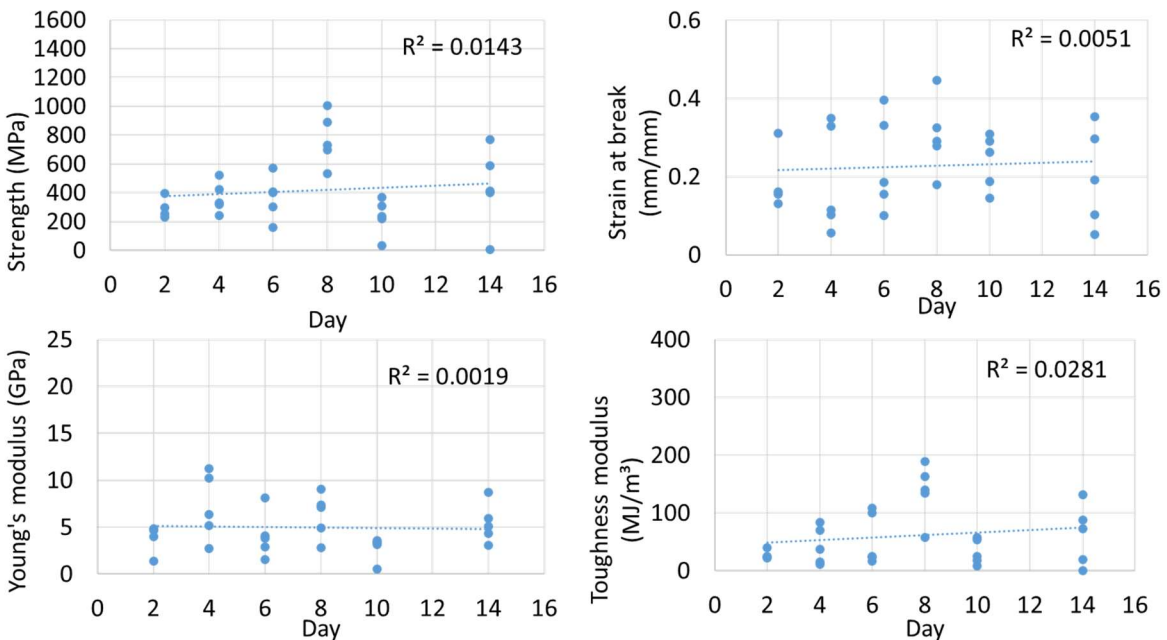
## Col samples



47  
48

Figure S9: All the mechanical properties of the Col line of spider silk. The dashed line represents the trend with its relative  $R^2$  value.

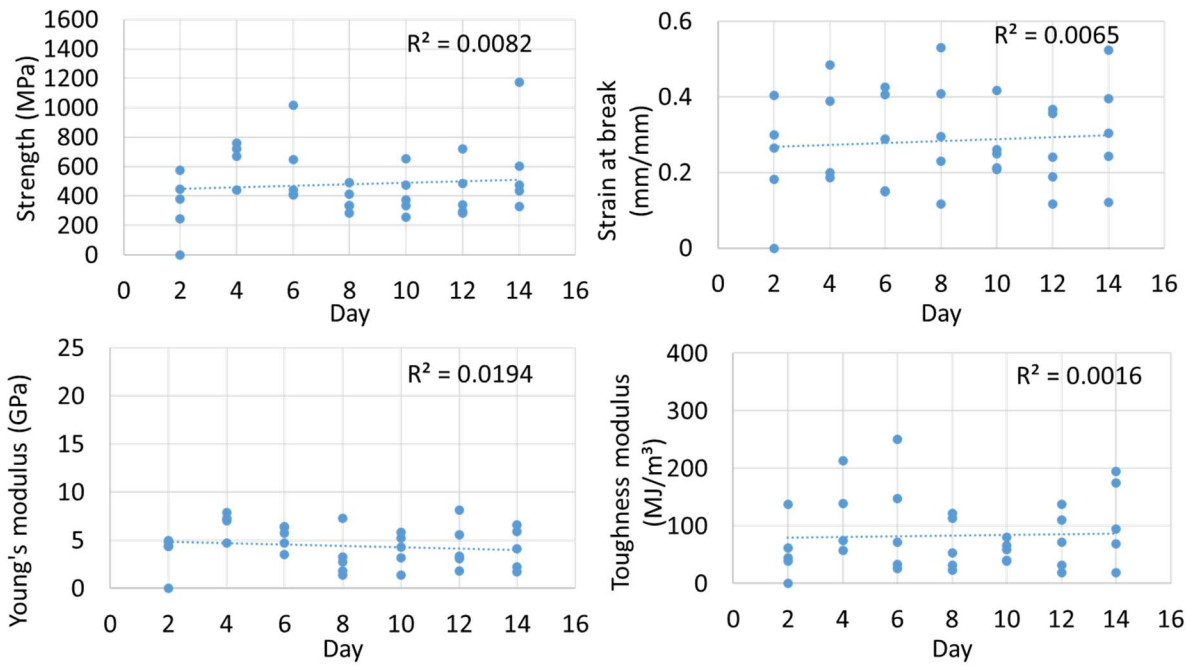
## C samples



49  
50

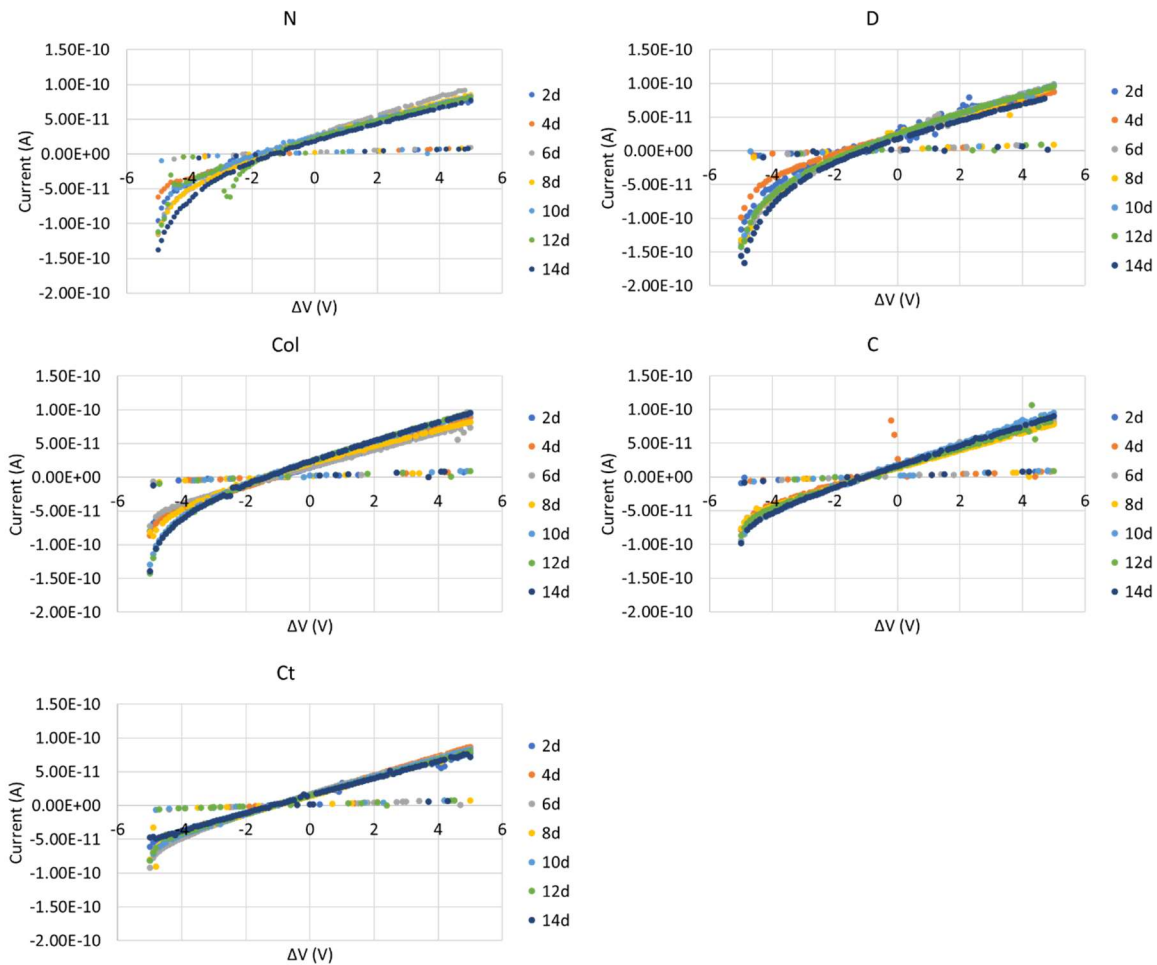
Figure S10: All the mechanical properties of the C line of spider silk. The dashed line represents the trend with its relative  $R^2$  value.

## Ct samples



51  
52

Figure S11: All the mechanical properties of the Ct line of spider silk. The dashed line represents the trend with its relative  $R^2$  value.



53

54

Figure S12: All the current Voltages curves for the spider silk fibers from different spider lines at different days.